Supporting Information

Transfer Hydrogenation and Antiproliferative Activity of Tethered Half-sandwich Organoruthenium Catalysts

Feng Chen,[†] Isolda Romero-Canelón,[†,‡] Joan J. Soldevila-Barreda,[†] Ji-Inn Song,[†] James P. C. Coverdale,[†] Guy J. Clarkson,[†] Jana Kasparkova,[§] Abraha Habtemariam,[†] Martin Wills,[†] Viktor Brabec[§] and Peter J. Sadler[*†]

[†] Department of Chemistry, University of Warwick, Gibbet Hill Road, Coventry CV4 7AL, U.K.

[‡] School of Pharmacy, Institute of Clinical Sciences, University of Birmingham, Birmingham B15 2TT, U.K.

[§] Institute of Biophysics, Academy of Sciences of the Czech Republic, Kralovopolska 135, CZ-61265 Brno, Czech Republic

Supporting Information

Tables S1 – S8 S2-S4

Figures S1 – S17 S5-S15

Table S1 Crystallographic Data for Complexes 1-4

	1	**2**	**3**	**4**
Crystal character	orange block	orange block	red block	red block
Formula	$C_{12}H_{19}ClN_2O_2RuS$	$C_{18}H_{23}ClN_2O_2RuS$	$C_{18}H_{20}ClF_3N_2O_2RuS$	$C_{17}H_{20}ClN_3O_4RuS$
FW	391.99	467.96	521.94	498.94
Temp (K)	150(2)	150(2)	150(2)	150(2)
Crystal system	triclinic	triclinic	monoclinic	monoclinic
Space group	P-1	P-1	$P2_{1/c}$	$P2_{1/c}$
a (Å)	8.0399(2)	9.9127(3)	10.4998(2)	10.5869(5)
b (Å)	11.6970(3)	10.3545(2)	16.9214(3)	16.4168(6)
c (Å)	16.8127(3)	10.6046(4)	11.6956(3)	11.4551(5)
α (°)	98.2250(17)	108.425(2)	90	90
β (°)	101.4472(18)	106.778(3)	111.867(3)	110.695(5)
γ (°)	106.688(2)	100.997(2)	90	90
Volume ($Å^3$)	1450.30(6)	939.87(5)	1928.47(7)	1862.48(15)
Z	2	2	4	4
Dcalc(mg/cm^3)	1.836	1.654	1.798	1.779
μ(mm^{-1})	1.412	1.101	1.105	1.127
F(000)	812.0	476.0	1048.0	1008.0
Crystal size (mm^3)	0.28 × 0.2 × 0.12	0.2 × 0.2 × 0.1	0.22 × 0.14 × 0.08	0.4 × 0.24 × 0.1
Reflections measured	44720	25185	32356	30846
Indep reflection	9700	6290	6963	6596
*R*1 [$I>2\sigma(I)$]	0.0318	0.0283	0.0255	0.0304
wR2 (all data)	0.1019	0.0611	0.1013	0.1167
CCDC no.	1823319	1823318	1823317	1823316

Table S2 Selected Hydrogen Bond Lengths (Å) and Angles (°) for Complex 1

D-H…A	D-H	H...A	D...A	< (DHA)	Symmetry operator
N106-H106...O1	1.00	2.16	3.020(3)	143.5	+X, +Y, 1+Z
N106-H106...Cl1	1.00	2.59	3.037(2)	107.3	1-X, 1-Y, -Z
N206-H206...O10A	1.00	2.26	3.001(3)	129.6	
N206-H206...Cl2	1.00	2.62	3.055(2)	106.4	
O1-H1A...Cl2	0.843(8)	2.509(12)	3.337(2)	167(4)	
O1-H1B...O20A	0.848(8)	1.974(13)	2.804(3)	166(4)	

Table S3 Selected Hydrogen Bond Lengths (Å) and Angles (°) for Complex 2

D-H…A	D-H	H...A	D...A	< (DHA)	Symmetry operator
N12-H12...Cl1	1.00	2.45	3.2678(14)	138.3	-x+1, -y+1, -z+1

Table S4 Selected Hydrogen Bond Lengths (Å) and Angles (°) for Complex 3

D-H…A	D-H	H...A	D...A	< (DHA)	Symmetry operator
N12-H12...Cl1	0.84(3)	2.60(3)	3.3080(17)	143(3)	1-X, 1-Y, 1-Z

Table S5 Selected Hydrogen Bond Lengths (Å) and Angles (°) for Complex 4

D-H…A	D-H	H...A	D...A	< (DHA)	Symmetry operator
N11-H11...Cl1	0.874(18)	2.55(3)	3.283(2)	143(3)	1-X, 1-Y, 1-Z
N11-H11...Cl1	0.874(18)	2.63(4)	3.037(2)	110(3)	-X, 1-Y, -Z

Table S6 Induction of ROS and Superoxide by Flow Cytometry Analysis of A2780 Ovarian Cancer Cells Exposed to Complex 2, Positive Control (Pyocyanin), or Negative Control. The Experiment Reads Superoxide in the FL2 Channel and Total ROS in the FL1 Channel.

Treatment	Cell Populations (%)			
	FL-1-/FL-2-	FL-1+/FL-2-	FL-1-/FL-2+	FL-1+/FL-2+
2	9 ± 1 **	82 ± 1 **	7.3 ± 0.2**	0.66 ± 0.09 **
Negative control	99.88 ± 0.04	0.10 ± 0.03	0	0.011 ± 0.002
Positive control	0.45 ± 0.08 **	1.5 ± 0.6 *	2.5 ± 0.9 **	96.1 ± 0.8 **

In all cases, independent two-sample *t*-tests with unequal variances, Welch's *t*-tests, were carried out to establish statistical significance of the variations against the negative control ($p < 0.01$ for **, and $p < 0.05$ for *).

Table S7 Cell Membrane Integrity by Flow Cytometry Analysis of A2780 Ovarian Cancer Cells Exposed to Complex 2 or Negative Control.

Treatment	Cell Population (%)	
	FL-1-	FL-1+
2	98.0 ± 0.2	2.6 ± 0.2
Negative control	98.6 ± 0.4	1.85 ± 0.5

Significance of the variations were carried out by Welch's *t*-tests, $^{**}p < 0.01$ and $^{*}p < 0.05$.

Table S8 Percentage of Cell Viability of A2780 Cells Exposed to Various Concentrations of Formate and a Fixed Concentration of Complexes 1-4.

Complex	Concentration of Formate			
	0 mM	0.5 mM	1.0 mM	2.0 mM
1	96 ± 2	91 ± 2	78 ± 3	74 ± 2
2	95 ± 2	96 ± 3	81 ± 4	78 ± 1
3	79 ± 2	75 ± 2	72 ± 3	63 ± 2
4	95 ± 1	88 ± 2	85 ± 2	81 ± 3

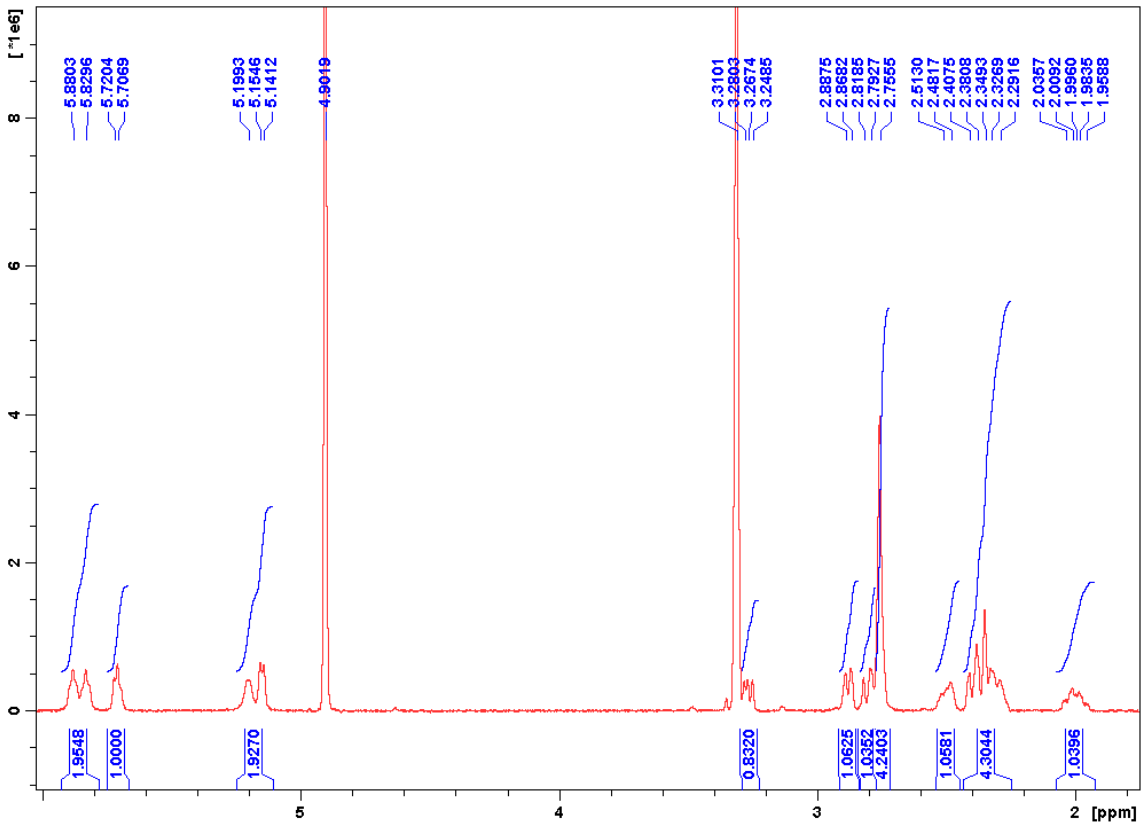

Figure S1 ^{1}H NMR spectrum of **1** in MeOD-d_4 (400 MHz).

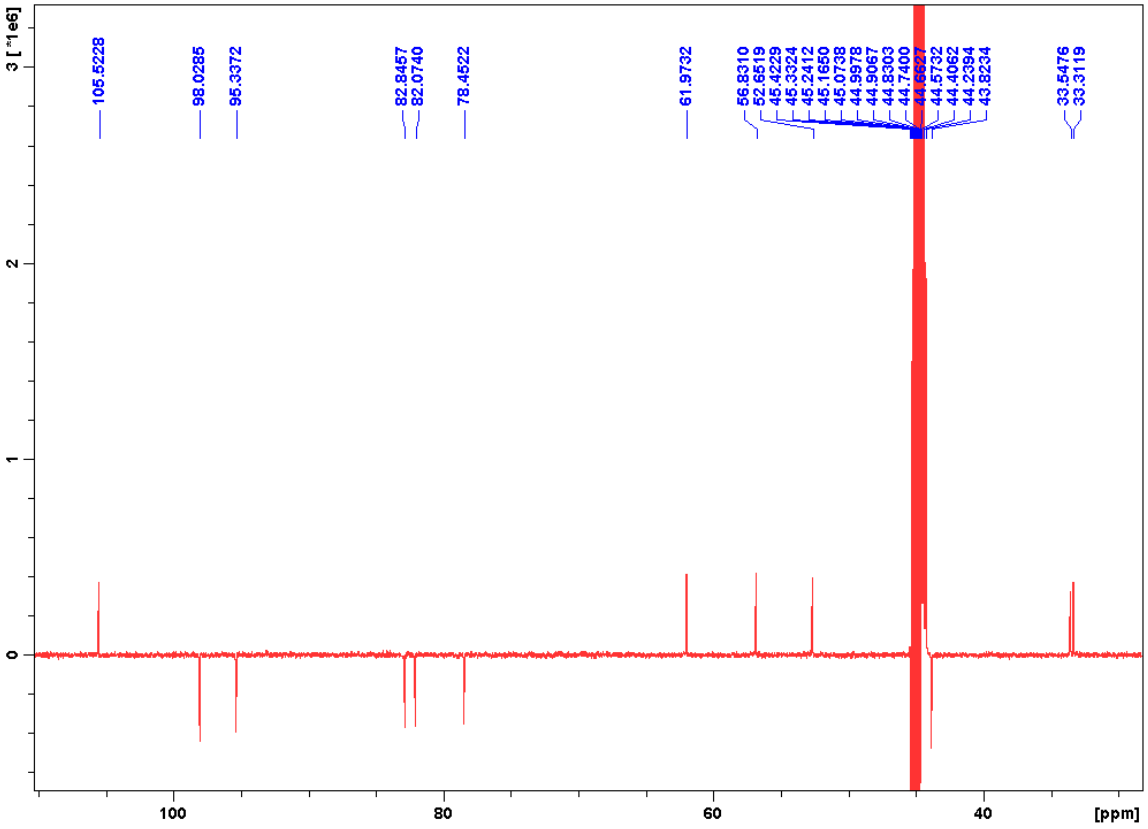

Figure S2 ^{13}C-APT NMR spectrum of **1** in DMSO-d_6 (125.7 MHz).

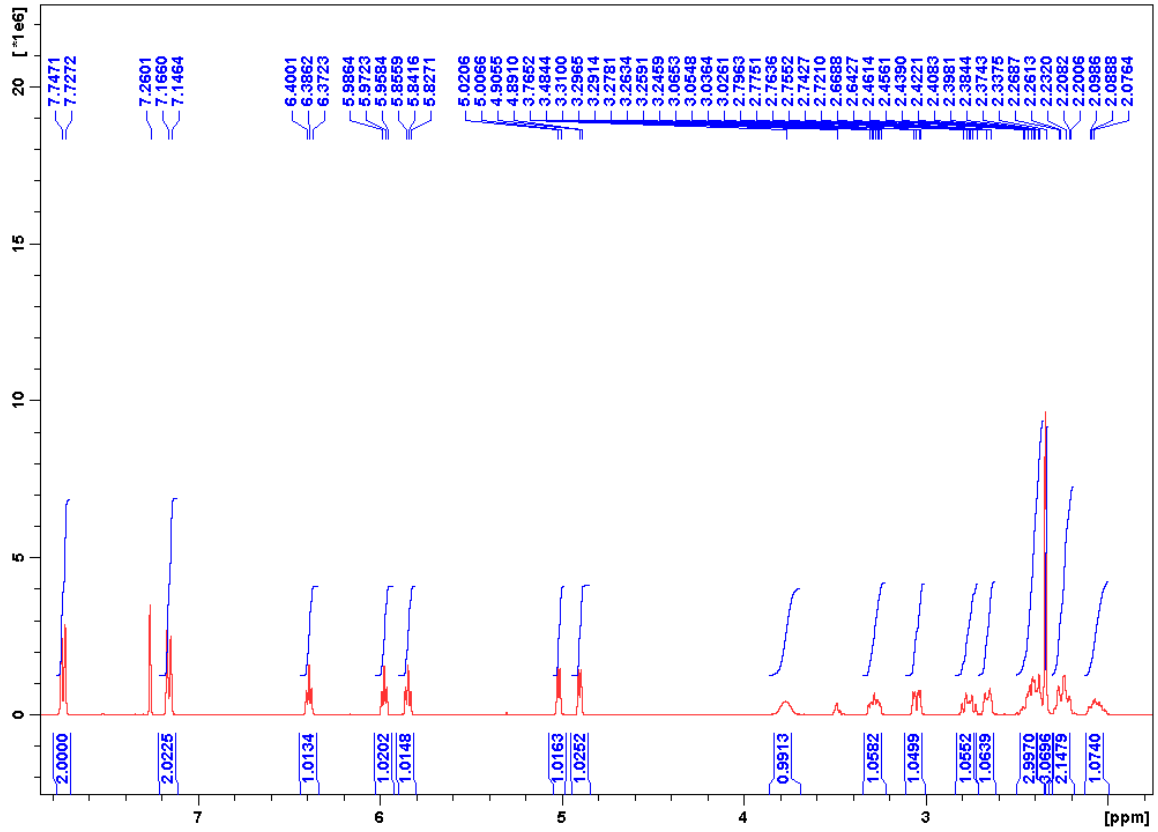

Figure S3 ^{1}H NMR spectrum of **2** in $CDCl_3$ (400 MHz).

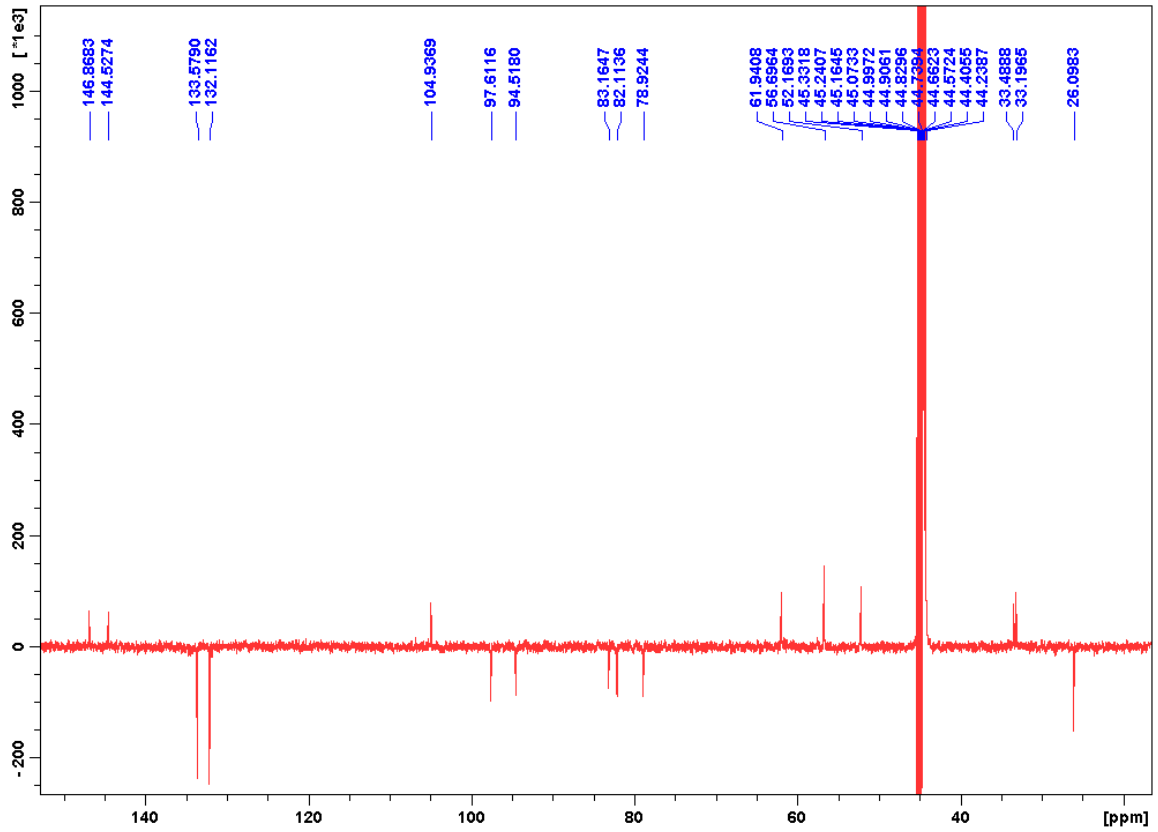

Figure S4 ^{13}C-APT NMR spectrum of **2** in DMSO-d_6 (125.7 MHz).

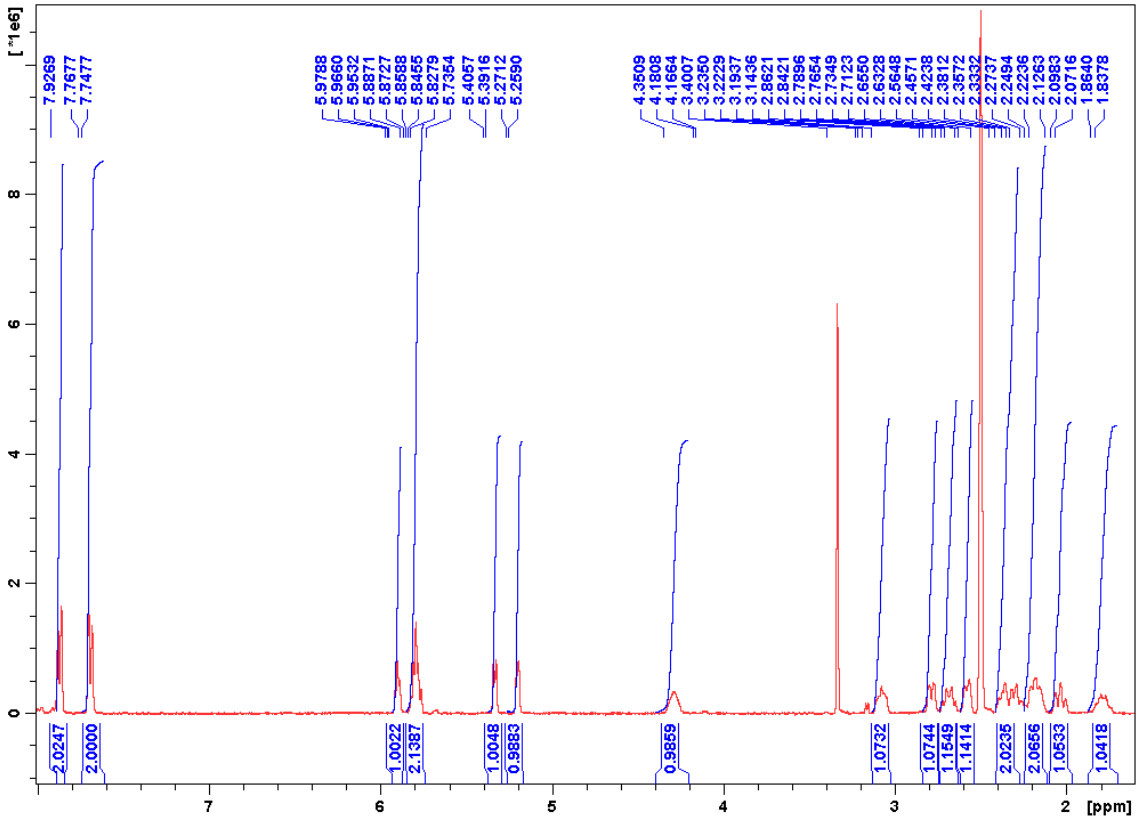

Figure S5 ^{1}H NMR spectrum of **3** in DMSO-d_6 (400 MHz).

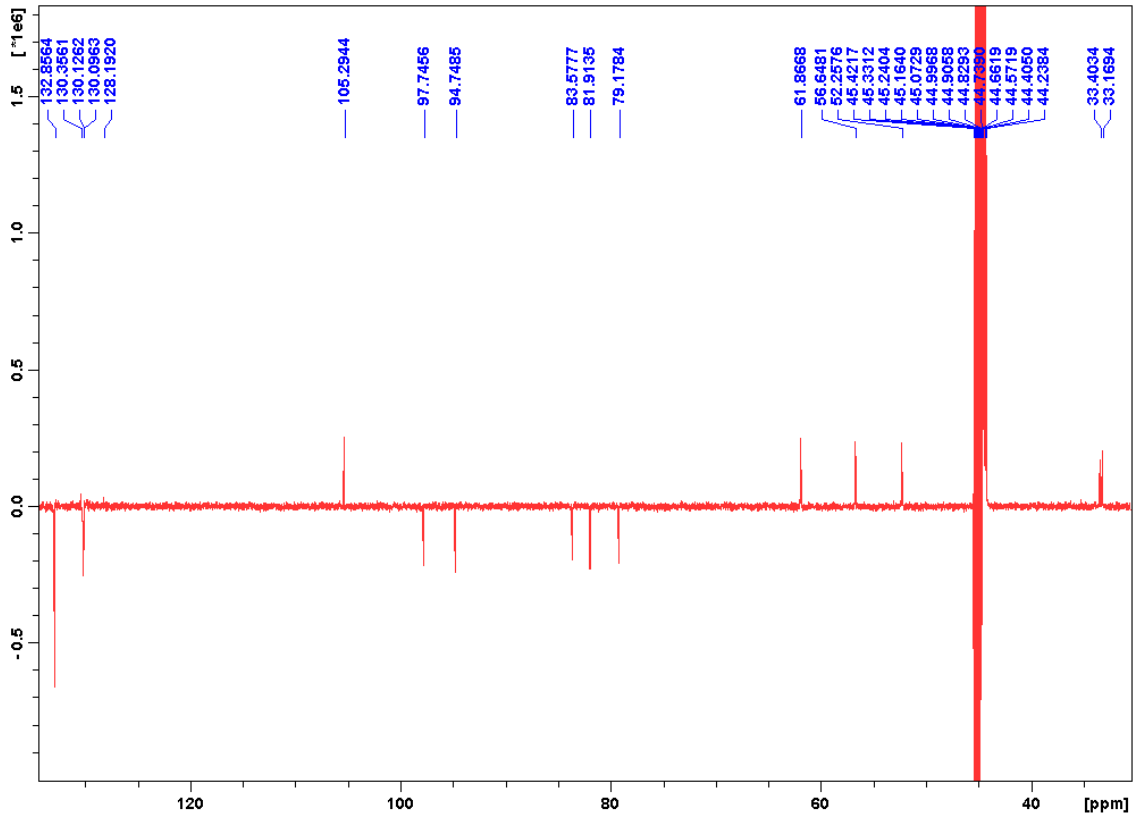

Figure S6 ^{13}C-APT NMR spectrum of **3** in DMSO-d_6 (125.7 MHz).

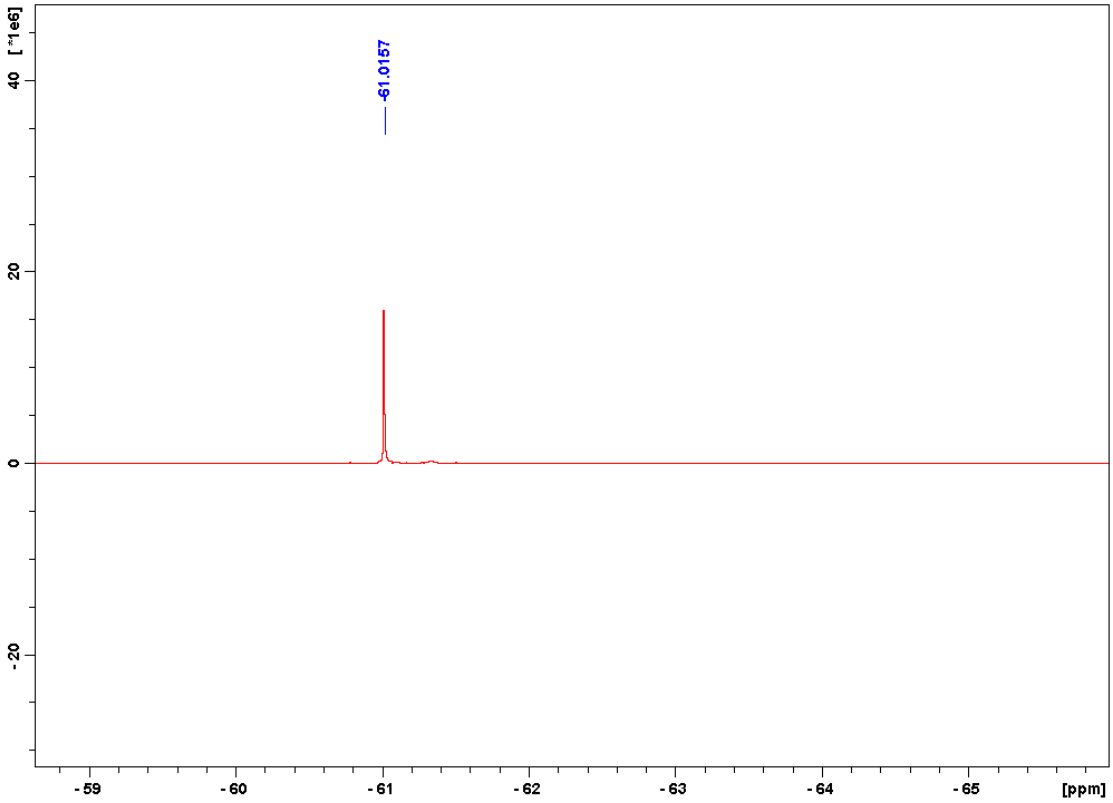

Figure S7 ^{19}F NMR spectrum of **3** in DMSO-d_6 (376.4 MHz).

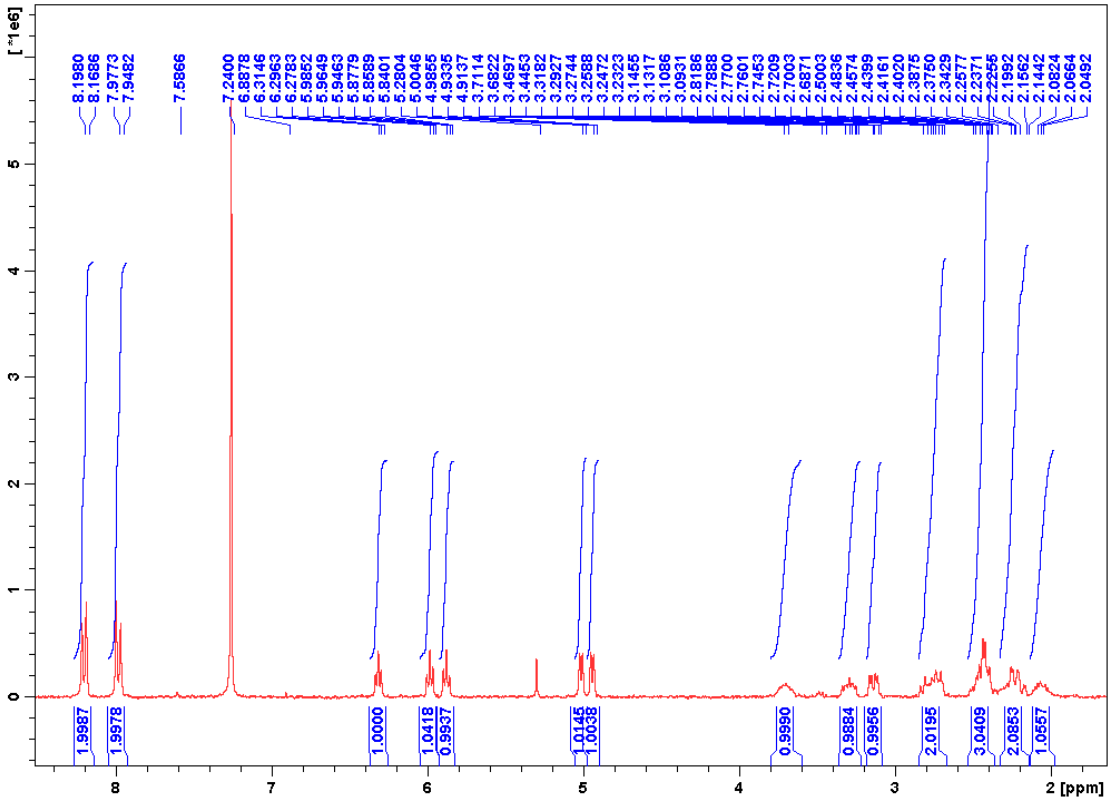

Figure S8 ^{1}H NMR spectrum of **4** in $CDCl_3$ (300 MHz).

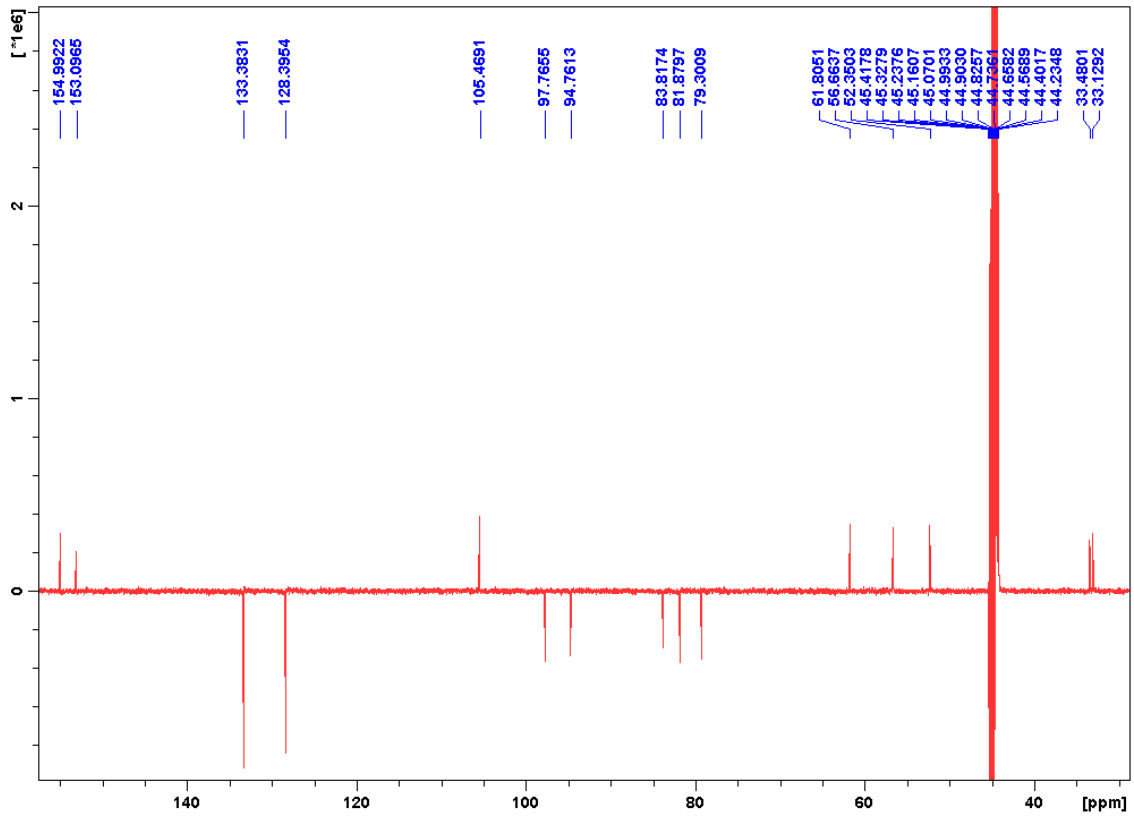

Figure S9 ^{13}C-APT NMR spectrum of **4** in DMSO-d_6 (125.7 MHz).

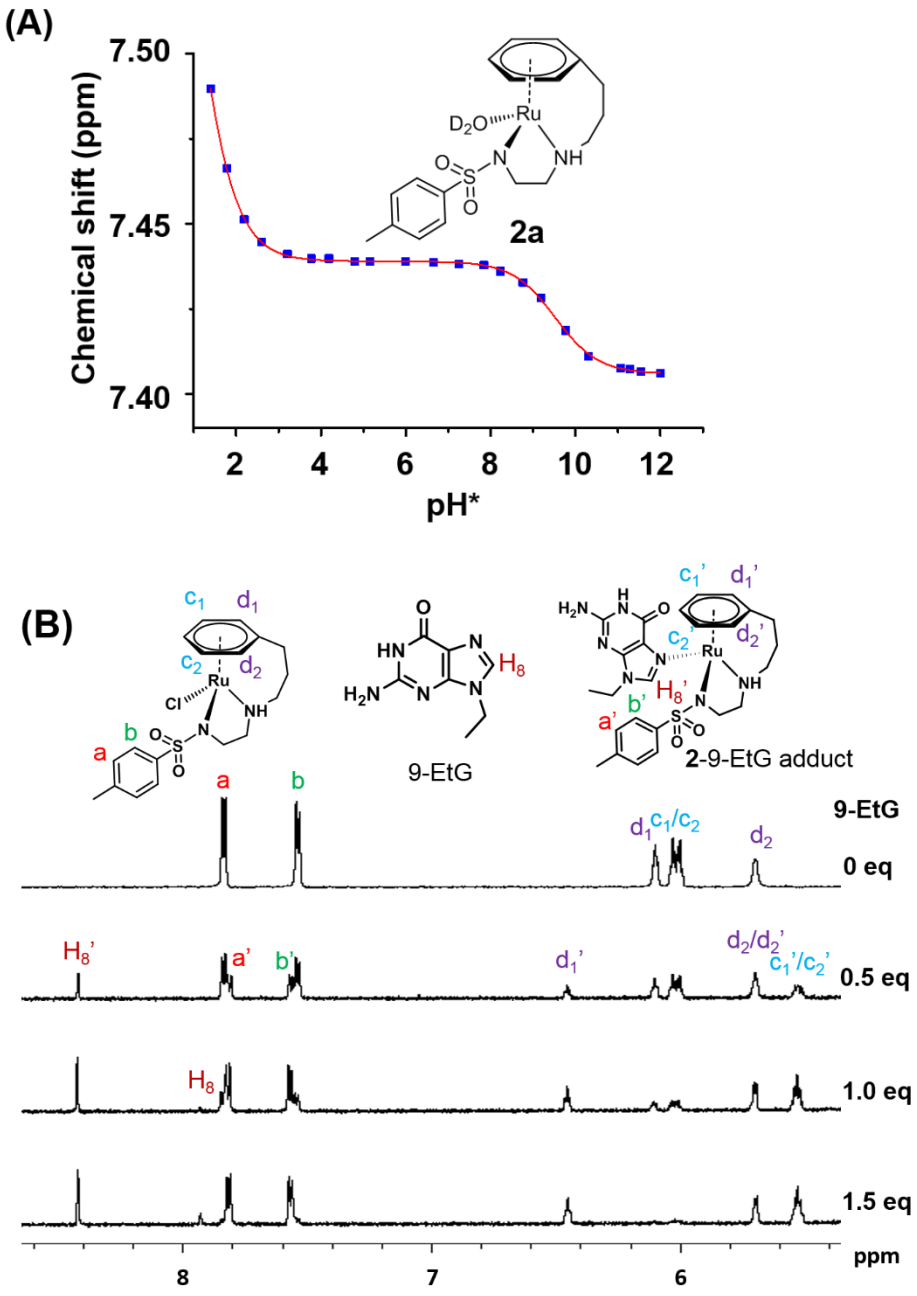
(A)
Chemical shift (ppm)
7.50
7.45
7.40
2
4
6
8
10
12
pH*
D2O
Ru
NH
2a
(B)
c1
d1
c2
d2
Cl
a
b
9-EtG
H8
c1'
d1'
c2'
d2'
H8'
b'
a'
2-9-EtG adduct
9-EtG
0 eq
d1
c1/c2
d2
H8'
a'
b'
d1'
d2/d2'
c1'/c2'
0.5 eq
H8
1.0 eq
1.5 eq
ppm
8
7
6

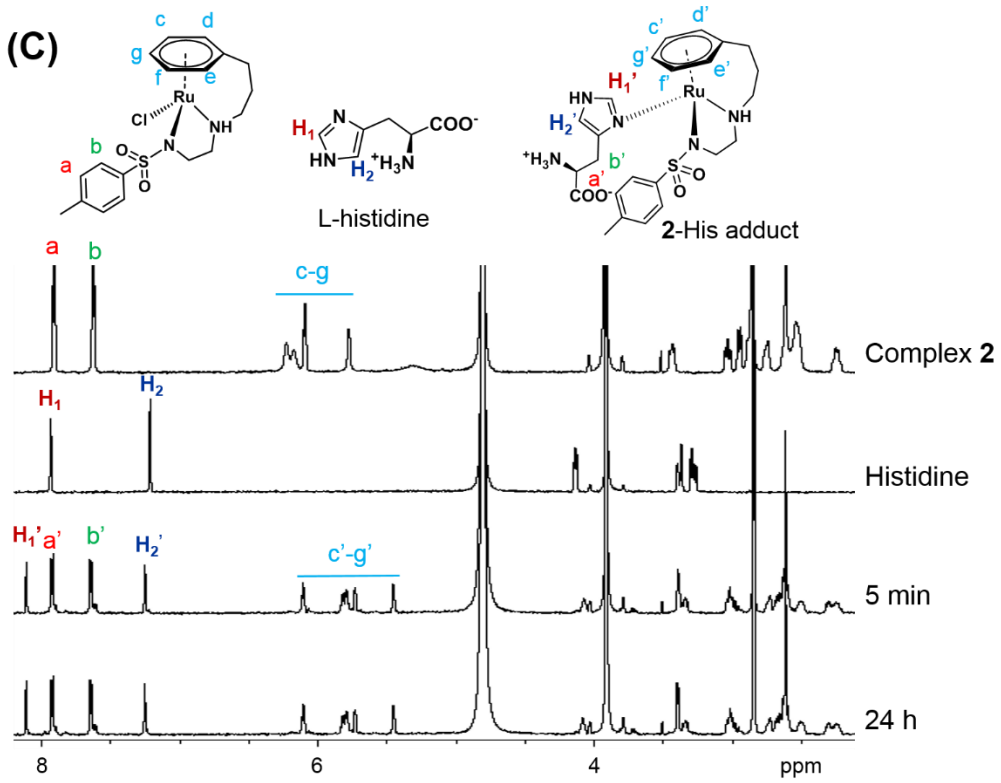

Figure S10 (**A**) Dependence of chemical shift of a low field ^{1}H NMR resonance (tosyl proton) of the aqua species **2a** on pH* showing the best fit corresponding to a pK_a* value of 9.52 for the coordinated water; (**B**) Titration of tethered Ru^{II} complex **2** (2 mM) with 9-ethylguanine (1 mM–3 mM, 0.5–1.5 molar equiv) in 10% MeOD-d_4/90% D_2O, pH at 7.2, 310 K, followed by ^{1}H NMR spectroscopy (spectra recorded ca. 10 min after mixing); (**C**) Reaction of complex **2** (2 mM in 20% MeOD-d_4/80% D_2O) with L-histidine (1 mol equiv) monitored by ^{1}H NMR at 310 K, pH* 7.1.

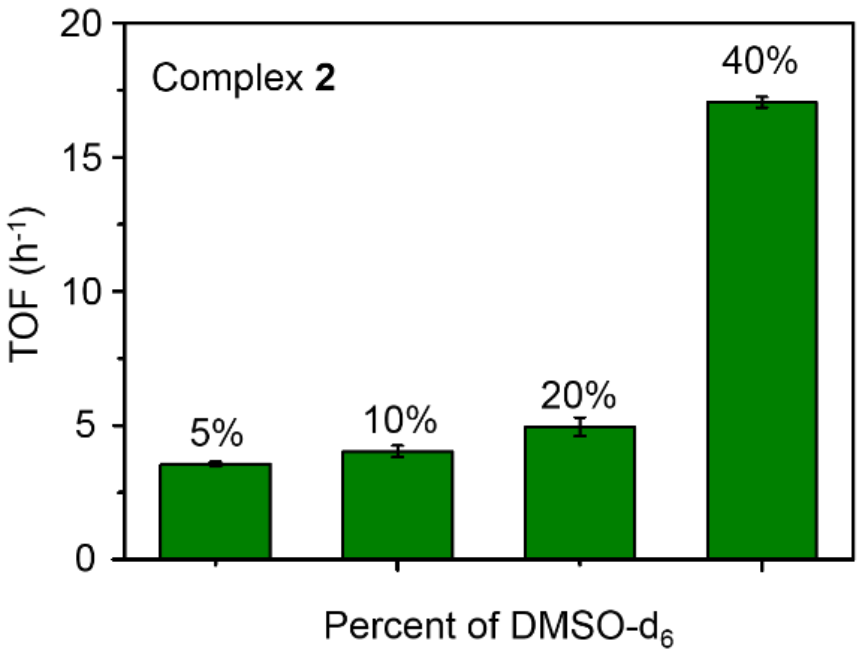

Figure S11 TOFs for TH reduction of NAD^+ by complex **2** as catalyst and sodium formate as hydride donor at 310 K, pH^* 7.1 in 5-40% v/v DMSO-d_6: D_2O mixtures monitored by 600 MHz ^1H NMR. With 80% DMSO, the reaction was too fast to follow.

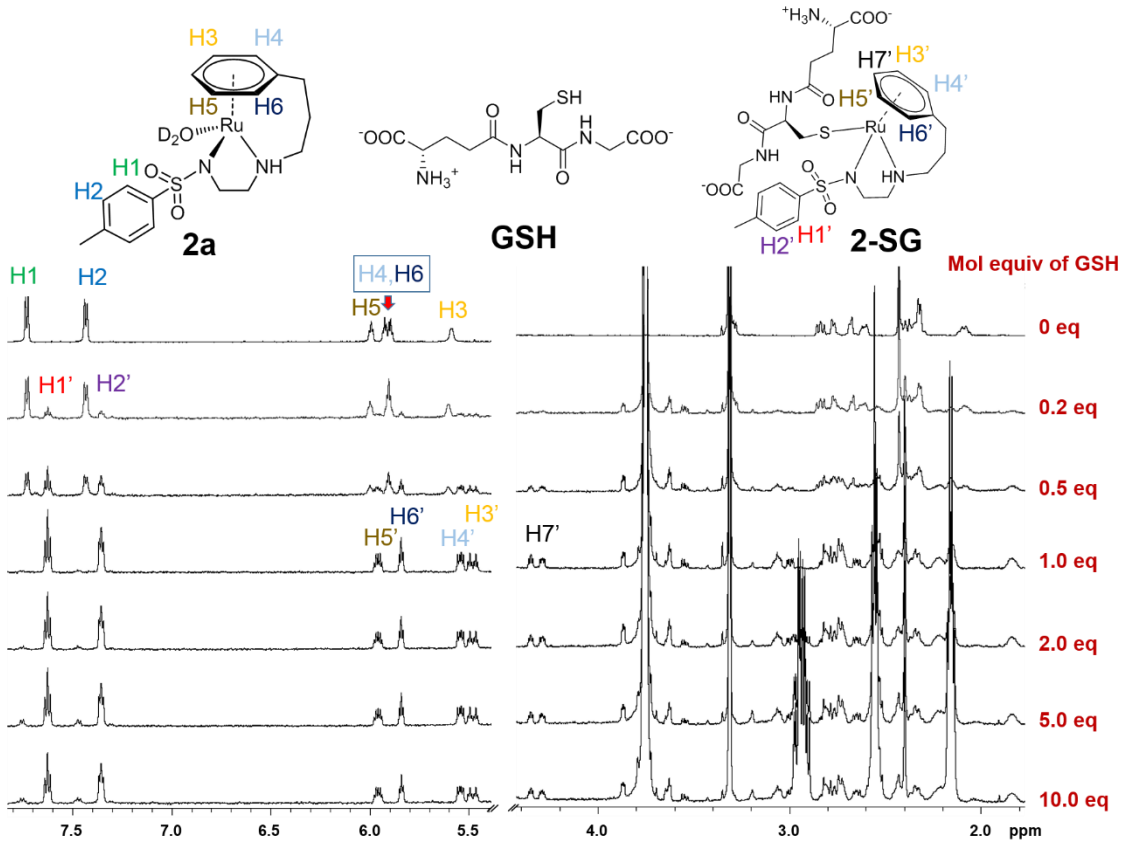

Figure S12 600 MHz ^{1}H NMR spectra monitoring of reactions between complex **2** (assigned as the aqua species **2a**, 2 mM in MeOD-d_4/D_2O, 1:9 v/v) and various concentrations of GSH in a mixture of MeOD-d_4 and D_2O (2:8, v/v), after *ca.* 10 min. The pH* was adjusted to 7.2 ± 0.1 and all spectra were recorded at 310 K. The **2**-SG complex appears as two diastereomers (e.g., 2 sets of H3´-H7´ peaks) and is fully formed in the presence of 1 mol equiv of GSH.

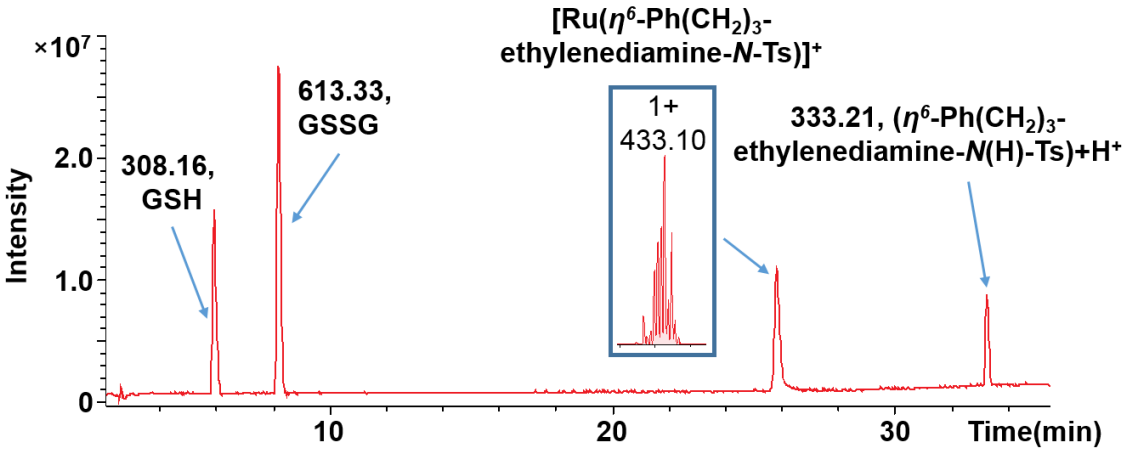

Figure S13 Reaction of complex **2** with GSH (10 mol equiv) in MeOH/H_2O (1:9, v/v) after incubation at pH 7.2, 310 K for 24 h monitored by LC-MS. Elution gradients are shown in Figure S14.

Time (min)	% B (acetonitrile, 0.1% TFA)
0	2
10	12
15	15
25	25
30	50
50	50
55	2

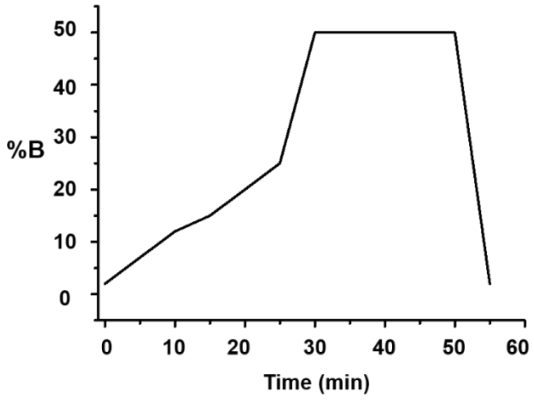

Figure S14 LC-MS gradients for identification of **2**-SG adducts from the reaction of complex **2** and GSH using H_2O with 0.1% TFA (v/v) (Solvent A) and CH_3CN with 0.1% TFA (v/v) (solvent B) as eluents (TFA, trifluoroacetic acid). Column type: ZORBAX Eclipse XDB-C18, 9.4 × 250 mm, 5 µm.

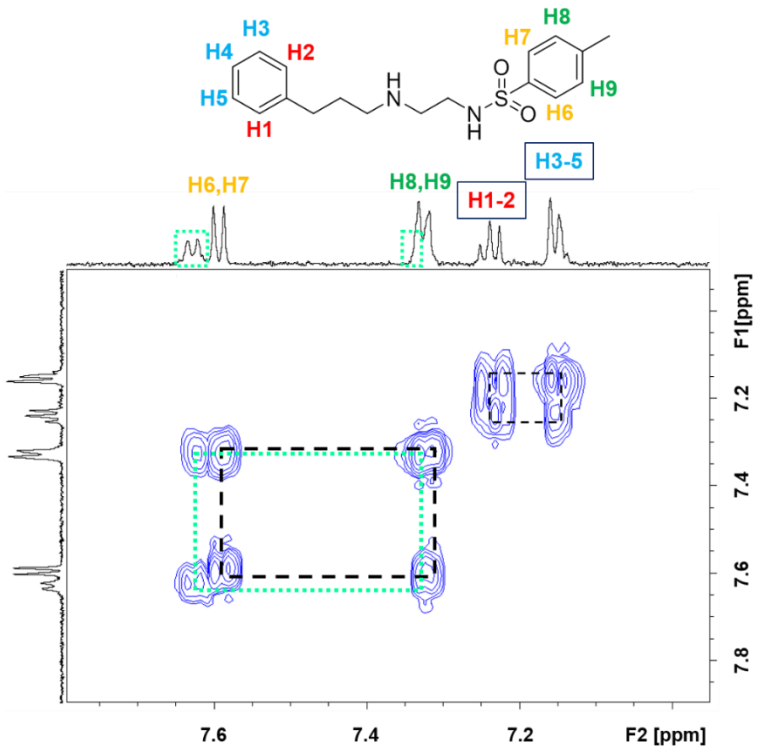

Figure S15 Low field region of a 2D COSY ^{1}H NMR spectrum showing peaks assignable to released free ligand η^6-Ph$(CH_2)_3$-ethylenediamine-*N*(H)-Ts (black dashed connector lines) detected for reaction of complex **2** (2 mM in MeOD-d_4/D_2O, 2:8, v/v) with GSH (20 mM, in D_2O) after 24 h incubation at 310 K. pH* was adjusted to 7.1. A second set of small peaks, possibly assignable to *p*-toluenesulfonate (arising from ligand hydrolysis), are connected by green dashed lines.

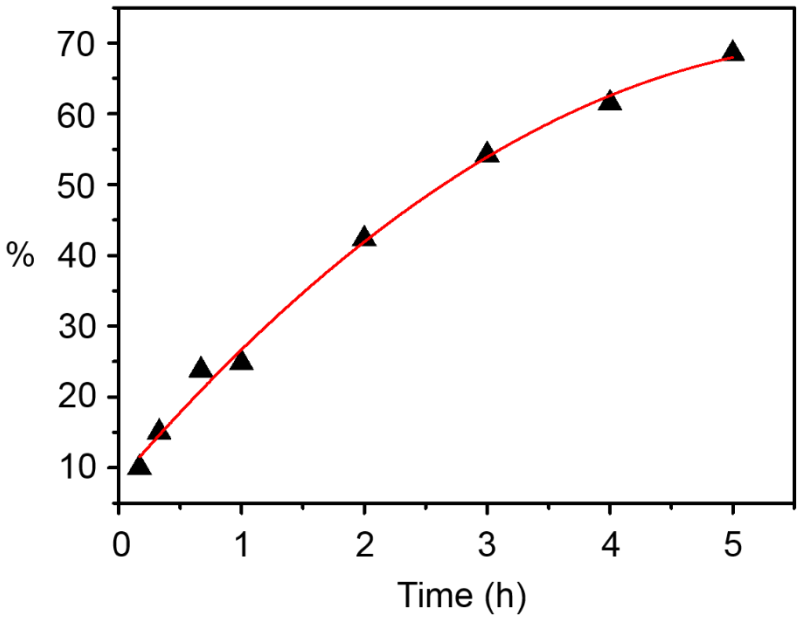

Figure S16 Percentage decomposition of glutathione complex **2**-SG and liberation of free ligand within 5 h for reaction of complex **2** (2 mM in MeOD-d_4/D_2O, 2:8, v/v) with GSH (20 mM, in D_2O) at pH^* 7.1, 310 K by ^1H NMR. Peak integration from **Figure 4**.

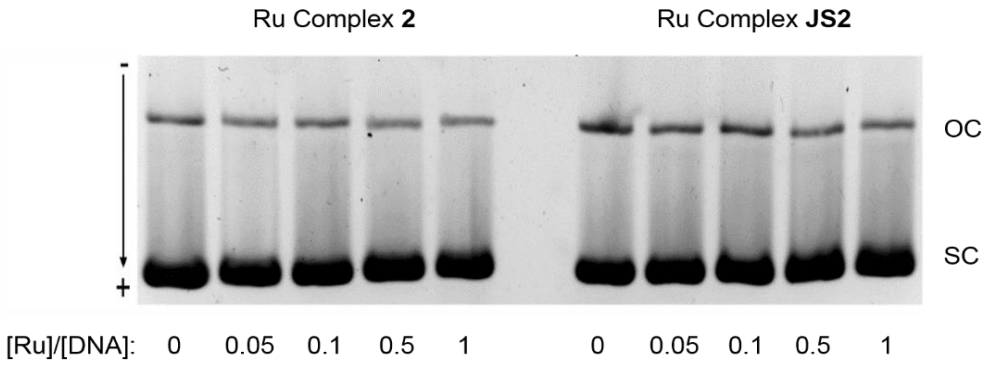

Figure S17 Interaction of complex **2** and **JS2** with bacterial plasmid DNA at various concentrations (r_i = 0-1). DNA samples were run on agarose gel followed by ethidium bromide staining. SC: supercoiled; OC: open circle. No significant changes of SC or OC were observed.